Fire Responses and Resistance of Concrete-Filled Steel Tubular Frame Structures

Min Yu[1], Xiaoxiong Zha[1], Jianqiao Ye[2,*] and Yi Li[1]

1. Shenzhen Graduate School, Harbin Institute of Technology, Shenzhen 518055, China;

2. School of Civil Engineering, the University of Leeds, Leeds, LS2 9JT, UK

Abstract: This paper presents the results of dynamic responses and fire resistance of concrete-filled steel tubular (CFST) frame structures in fire conditions by using non-linear finite element method. Both strength and stability criteria are considered in the collapse analysis. The frame structures are constructed with circular CFST columns and steel beams of I-sections. In order to validate the finite element solutions, the numerical results are compared with those from a fire resistance test on CFST columns. The finite element model is then adopted to simulate the behaviour of frame structures in fire. The structural responses of the frames, including critical temperature and fire-resisting limit time, are obtained for the ISO-834 standard fire. Parametric studies are carried out to show their influence on the load capacity of the frame structures in fire. Suggestions and recommendations are presented for possible adoption in future construction and design of these structures.

Keywords: Column**,** concrete-filled steel tube, frame, fire resistance, strength and stability under fire condition, finite element method.

1 Introduction

Concrete filled steel tubular (CFST) structures, which are produced by filling concrete into steel tubes, are now increasingly used in fireproof design of structures due to their favourable fire resistance (Ding and Wang[1], Kim et al[2], Kvedaras and Sapalas[3], O'Meagher et al[4], Okada[5],). Researchers have carried out extensive theoretical and experimental investigations on fire resistance of CFST columns. Lie studied the fire resistance of CFST for both plain and reinforced concrete by tests (Lie[6], Lie and Stringer[7],). Kodur[8] presented simplified formulas that can be used to calculate fire-resisting limit of circular and square CFST. The formulas were

* Correspondence authors: j.ye@leeds.ac.uk, X.X.Zha:zhaxx@hit.edu.cn

verified by experiments in Kodur[8]. It was also found in Lie[6] and Lie and Stringer[7] that in general high-strength CFST columns could not satisfy the requirement of fire-resisting limit. In order to improve their fire-resisting limit, steel fibres or steel reinforcements can be added into high-strength concrete (Kodur and Sultan[9]). Wang[10-11] , Zha[12] , Liu[13] and Yin, et al[14] studied fire-resisting limit of CFST members by finite element method. Han[15] and Han et al[16-18] carried out a series of studies on CFST members through experiments and theoretical analysis. They proposed a method to compute the thickness of fire protection layer that has now been used in the practical design. However, most of these studies were focused on investigating fire resistance of single components. Limited work was reported in the literature on fire resistance of integrated frame structures. These include a research report published by the University of Edinburgh on fire resistance of steel frame structures, in which global fire resistance of floor slabs with both transverse and longitudinal support beams was analysed (University of Edinburgh[19]). Wang[20] studied fire-resisting limit of CFST columns with different boundary conditions and the influence of beams of a frame structure on the fire resistance of CFST columns. In fact, fire resistance of an individual CFST column is different from that of the same column as an integrated member of a frame. Thus, it is practically important to study the fire resistance behaviour of a CFST column that is interactive with other members of the frame.

A CFST column is normally considered to be exposed to all-around fire when its fire resistance is studied. In some situations, however, a CFST column may be exposed to one-sided fire, such as columns joined with a fire division wall. When a CFST column is exposed to one-sided fire, the axial expansion of the column is not uniform. This leads to an initial bending of the column that pushes the column to deflect towards the wall.

In this study, the finite element method is used to simulate fire resistance analysis of CFST frame structures. The numerical modelling is validated first through comparisons with test results of CFST columns. In the calculations, CFST columns exposed to one-sided and all-around fires are both considered. The comparisons between these two groups of results are presented. The fire resistance of both CFST columns in a frame and single CFST columns under the same thermal and mechanical conditions are then calculated and compared.

2 Validation of the finite element model

2.1 The test results

The fire resistance tests of concrete-filled steel tubes bearing axial compression are detailed in Lie[6] and Lie and Stringer[7] , where the steel tubes filled with both plain and reinforced concrete were tested. The tests conducted at the National Fire Laboratory, Institute for Research in Construction in Canada (Lie and Stringer[7]), were full size tests on fire resistance of hollow steel columns filled with plain concrete bearing axial compression. Two of the tests are selected here to validate the feasibility of the finite-element modelling.

The fire resistance tests were carried out in a furnace. The average temperature in the furnace was in accordance with ASTM-E119 standard temperature-time relation that was defined by a series of discrete points in the temperature-time co-ordinates. The columns were fixed at both ends against rotation. The height of the columns was 3810mm. The sections of the two steel tubes were: 273.1mm x 5.56mm for column (a) and 219.1mm x 4.78mm column (b). The yield strength of the steel was 350MPa. The strength of the concrete was 30MPa at the time of the test. The respective axial loads applied at the top end of the columns were 525kN and 492kN, which were about 14.8% and 23.1% of the axial load bearing capacity. Fire-resisting limit times were 133 minutes and 80 minutes, respectively.

2.2 Material parameters

For the heat transfer calculations, the thermal properties of steel and concrete in Lie and Stringer[7] are used since these parameters include the effects of water in concrete on heat transfer.

A: Thermal properties of steel

a. Conductivity of steel, k_s , is:

$$\begin{cases} 0^oC \le T \le 900^oC: & k_s = -0.022T + 48 & [W/(m^oC)] \\ T > 900^oC: & k_s = 28.2 & [W/(m^oC)] \end{cases} \tag{1}$$

where T denotes temperature of steel.

b. Specific heat capacity of steel, c_s, is defined by:

$$\begin{cases} 0^oC \le T \le 650^oC: & \rho_s c_s = (3.3 + 0.004T) \times 10^6 & [J/(m^3\,{}^oC)] \\ 650^oC < T \le 725^oC: & \rho_s c_s = (0.068T - 38.3) \times 10^6 & [J/(m^3\,{}^oC)] \\ 725^oC < T \le 800^oC: & \rho_s c_s = (-0.086T + 73.35) \times 10^6 & [J/(m^3\,{}^oC)] \\ 800^oC < T: & \rho_s c_s = 4.55 \times 10^6 & [J/(m^3\,{}^oC)] \end{cases} \quad (2)$$

where ρ_s is the density of steel, and takes $\rho_s = 7850 kg/m^3$ in the calculation.

c. Coefficient of thermal expansion of steel, α_s, is:

$$\begin{cases} 0^oC \le T < 1000^oC: & \alpha_s = (0.004T + 12) \times 10^{-6} & [m/(m^oC)] \\ T \ge 1000^oC: & \alpha_s = 16 \times 10^{-6} & [m/(m^oC)] \end{cases} \quad (3)$$

B: Thermal properties of concrete

a. Conductivity of concrete, k_c, is:

$$\begin{cases} 0^oC \le T \le 293^oC: & k_c = 1.355 & [W/(m^oC)] \\ T > 293^oC: & k_c = 1.7162 - 0.001241T & [W/(m^oC)] \end{cases} \quad (4)$$

where T is the temperature of concrete.

b. Specific heat capacity of concrete, c_c, follows:

$$\begin{cases} 0^oC \le T \le 400^oC: & \rho_c c_c = 2.566 \times 10^6 & [J/(m^{3o}C)] \\ 400^oC < T \le 410^oC: & \rho_c c_c = (0.1765T - 68.034) \times 10^6 & [J/(m^{3o}C)] \\ 410^oC < T \le 445^oC: & \rho_c c_c = (-0.05043T + 25.00671) \times 10^6 & [J/(m^{3o}C)] \\ 445^oC < T \le 500^oC: & \rho_c c_c = 2.566 \times 10^6 & [J/(m^{3o}C)] \\ 500^oC < T \le 635^oC: & \rho_c c_c = (0.01603T - 5.44881) \times 10^6 & [J/(m^{3o}C)] \\ 635^oC < T \le 715^oC: & \rho_c c_c = (0.16635T - 100.90225) \times 10^6 & [J/(m^{3o}C)] \\ 715^oC < T \le 785^oC: & \rho_c c_c = (-0.22103T + 176.07343) \times 10^6 & [J/(m^{3o}C)] \\ 785^oC < T: & \rho_c c_c = 2.566 \times 10^6 & [J/(m^{3o}C)] \end{cases} \quad (5)$$

where ρ_c is the density of desiccated concrete, and takes $\rho_c = 2350 kg/m^3$.

In order to consider the influence of water, the following modifications to Equation 5 were suggested by Lie and Stringer[7].

$$\begin{cases} 100^oC > T: \ \rho'_c c'_c = 0.95\rho_c c_c + 0.05\rho_w c_w \\ 100^oC \le T: \ \rho'_c c'_c = \rho_c c_c \\ \rho_w c_w = 4.2\times 10^6 \quad \left[J/(m^{3o}C) \right] \end{cases} \tag{6a}$$

where c_w and c'_c are the respective specific heat capacity of water and concrete containing water; ρ_w is the density of water; ρ'_c is the density of concrete containing water. In the simulation,

$$\rho'_c = 2350 kg/m^3 \qquad T < 100^oC$$

$$c'_c = \left(0.95\rho_c c_c + 0.05\rho_w c_w\right)/\rho'_c = 1127\ J/(kg^oC) \tag{6b}$$

c. Coefficient of thermal expansion of concrete, α_c, is:

$$\alpha_c = (0.008T + 6)\times 10^{-6}\left[m/(m^oC) \right] \tag{7}$$

C: Mechanical properties of steel under high temperature

The bilinear constitutive law of steel (Figure 1) is used in the calculation.

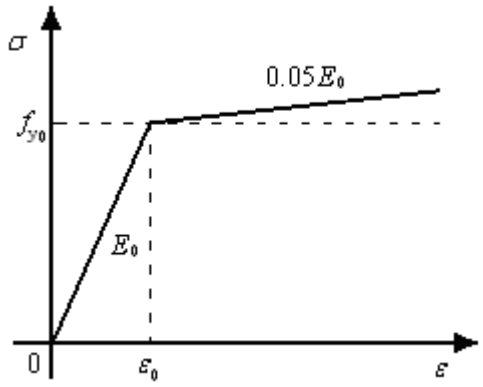

Figure 1: The constitutive relation of steel

Figure 1 shows the strain stress relationship of steel subject to a temperature of 20^{o}C. The instantaneous elastic modulus of the steel reduces as the temperature increases. The ratio of the instantaneous elastic modulus and the modulus at 20^{o}C follows the equation below (Li[21]).

$$\frac{E}{E_0}=\begin{cases}1-\dfrac{13(T-20)}{33000} & 20^oC\le T\le 350^oC\\ 0.87-\dfrac{57(T-350)}{25000} & 350^oC\le T\le 600^oC\\ 0.3-\dfrac{3(T-600)}{4000} & 600^oC\le T\le 1000^oC\end{cases} \tag{8}$$

where E_o is the elastic modulus at 20^oC.

The instantaneous yield strength of steel, f_y, also reduces as the temperature increases and is as follows:

$$\frac{f_y}{f_{y0}}=\begin{cases}1-\dfrac{13(T-20)}{18000} & 20^oC\le T\le 200^oC\\ 0.87-\dfrac{7(T-200)}{3500} & 200^oC\le T\le 550^oC\\ 0.17-\dfrac{17(T-550)}{45000} & 550^oC\le T\le 1000^oC\end{cases} \tag{9}$$

where f_{y0} is the yield strength at 20^oC.

D: Mechanical properties of concrete subject to high temperature

The material specifications adopted in the Eurocode are used in the calculation for concrete. The constitutive law of concrete is shown in Figure 2, including a nonlinear ascending phase and a linear descending phase in compression (EN 1994-1-2:2005[22]), and a modified strain-stress relation in tension. In the tension zone, the ultimate tensile strength $f_{t,T}=0.1f_{c,T}$.

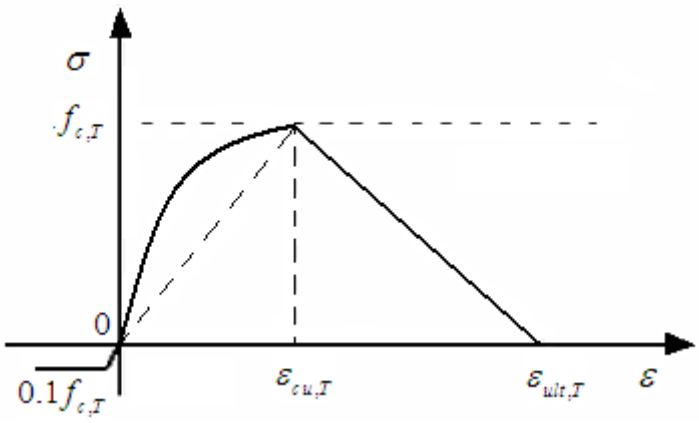

Figure 2: The constitutive relation of concrete

The material properties of the concrete shown in Figure 2 are taken as temperature dependent and the temperature dependent properties are presented in Table 3.1.

Table 3.1 Material properties of concrete vs. temperature variation

T [^oC]	$k_{c,T} = f_{c,T} / f_c$	$\varepsilon_{cu,T} \times 10^3$	$\varepsilon_{ult,T} \times 10^3$
20	1.0	2.5	20.0
100	0.95	3.5	22.5
200	0.90	4.5	25.0
300	0.85	6.0	27.5
400	0.75	7.5	30.0
500	0.60	9.5	32.5
600	0.45	12.5	35.0
700	0.30	14.0	37.5
800	0.15	14.5	40.0
900	0.08	15.0	42.5
1000	0.04	15.0	45.0
1100	0.01	15.0	47.5
1200	0.0	15.0	50.0

It is recognized that the creep of concrete and steel subject to elevated temperature is a very complex issue that has attracted substantial research in this special field. Since creep is not a dominating factor in a fire resistance analysis, it is ignored in the following study.

2.3 Finite element model

2.3.1 Basic assumptions in the FEM analysis

In order to simulate a CFST column in fire using the finite element method, the following assumptions are introduced to maximize the efficiency of numerical procedure with acceptable loss of accuracy.

A: No relative slip and separation between concrete and steel tube.

Under this assumption the finite element is continuous across the steel and concrete boundaries and there is no need to introduce contact interfaces between the element nodes of the two materials. As a result, thermal flow can be imported directly through the continuous nodes in

the FEM and the mechanical analysis is also significantly simplified. Though, the steel tube may buckle locally in fire and tend to break away from the concrete, this alters only the distribution of the local thermal field. Due to the triaxial pressure, it has been observed that before failure occurs, the concrete always occupies fully the entire hollow space of the steel tube which suggests that this assumption will not introduce significant errors.

B: No abruption in concrete.

Since the major type of collapse is buckling, assuming that there is no abruptions in concrete can simplify the finite element analysis, and this also in agreement with the first assumption.

C: No coupling of strain and temperature

In the heating processes, a significant temperature gradient and restricted thermal expansion caused by this temperature gradient are generated. As a result, thermal stress is generated in the column, and the influence of temperature field to the stress field is considered.. Due to the fact that the deformation of the column is very small, the influence of the stress/strain field on the temperature field is ignored in this paper. However, the influence of the stress/strain on temperature must be considered when the deformation has great influence on heat flux (Duan[23])

D: No creep and transient deformations.

Because the deformation is mainly due to mechanical and thermal loads, creep and transient deformations are sufficiently small, this paper ignores these two deformations to simplify the analysis.

2.3.2 Thermal transfer and contact

In the calculation, it is assumed that heat is transferred to the surface of the column from fire by convection and radiation. It follows:

$$q = h(T_f - T_s) + \varepsilon\sigma(\theta_f^4 - \theta_s^4) \tag{10}$$

Where q is the heat flux on the column surface; h is the heat transfer coefficient for convection, given as 25 $W/(m^{2o}C)$; T_f is the relative temperature of fire and T_s the relative surface temperature of the column; θ_f is the absolute temperature of fire and θ_s the absolute surface

temperature of column; ε denotes emissivity, taken as 0.7; and σ is the Boltzmann constant, taken as $5.67\times10^{8} W/m^{2}T^{4}$.

Inside the column, the main channel of heat transfer is conduction. At the interface of the steel tube and the concrete, heat transfer is rather complex due to the rough contact. Although perfect bond between the steel tube and the concrete core is assumed, thermal resistance exists at the interface due to different thermal properties of the materials. Thermal contact was then introduced in the simulations. The conductivity between the two materials is presented in the following simplified form:

$$\begin{aligned} q &= \alpha(T_t - T_c) \\ \alpha &= \sqrt{kc_c\rho_c / \pi t} \end{aligned} \tag{11}$$

where α is the heat release coefficient; k is the heat transfer coefficient of steel and t denotes time in hour. T_s is the inner surface temperature of the steel tube; T_c is the surface temperature of the concrete;

For the purpose of comparisons, the average temperature in the furnace of the tests was in accordance with ASTM-E119 standard temperature-time relation, from which, a heating-up curve and its expression were proposed by Lie[6]. The curve was then adopted by CAN4-S101 and the expression is as follows:

$$T = T_0 + 750[1 - \exp(-3.79533\sqrt{t})] + 170.4\sqrt{t} \tag{12}$$

where T_0 is the initial temperature of the test and is assumed 20^{o}C in the finite element analysis.

2.3.3 The finite element simulation process

The finite element software used in this research is ABAQUS. It is one of the most powerful finite element analysis packages available today, and can solve various non-linear problems. In this study, two major steps are followed: The temperature field of the CFST columns under fire is calculated first. The mechanical behaviour of the CFST columns due to the temperature field is then studied.

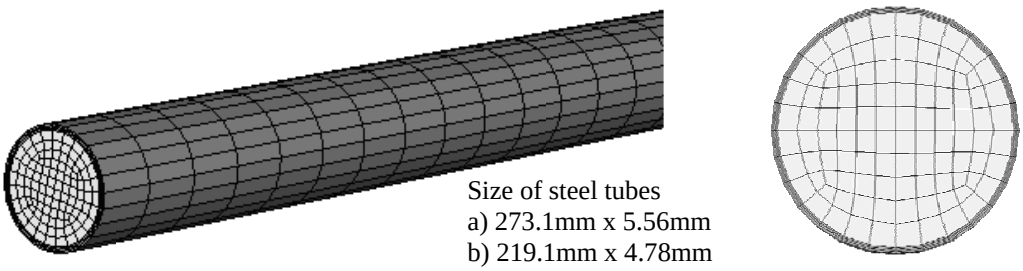

Figure 3: Finite element model of CFST column

In the finite element analysis, 3D solid elements are used for both the steel tube and the concrete. The finite element model and meshes are shown in Figure 3.

In the first step, the heat transfer problem is solved by employing the DC3D8 element for both the steel and concrete. The thermal heating load is defined according to the curve used in the experiment (Equation 12). The thermal contact between the concrete and the steel tube is specified by assumption A (Equation 11).

In the second step, mechanical loads and boundary conditions are added to the model. The bottom end of the column is defined as fixed. The degrees of freedom of the top end are suppressed except the vertical displacement. The C3D8R element is now used for both the steel tube and the concrete. Subjected to the temperature field from the first step, the vertical head displacement of the CFST column is obtained.

In order to assess the influence of meshing on the computed temperature field and the vertical head displacement, three different meshing schemes are followed to analyze CFST column (b). They are:

Mesh one: The column is divided into 30 segments along the axis direction. The cross section is divided into 84 steel and 104 concrete elements, respectively;

Mesh two: The column is divided into 60 segments along the axis direction. The cross section is divided into 84 steel and 104 concrete elements, respectively;

Mesh three: The column is divided into 60 segments along the axis direction. The cross section is divided into 84 steel and 204 concrete elements, respectively.

The comparisons of the temperature fields and vertical head displacements computed from the three meshes are shown in Figure 4. The temperature fields are virtually identical and the vertical head displacements show excellent agreement. On the basis of the comparison, meshing scheme one is selected to obtain all the results in the following calculations.

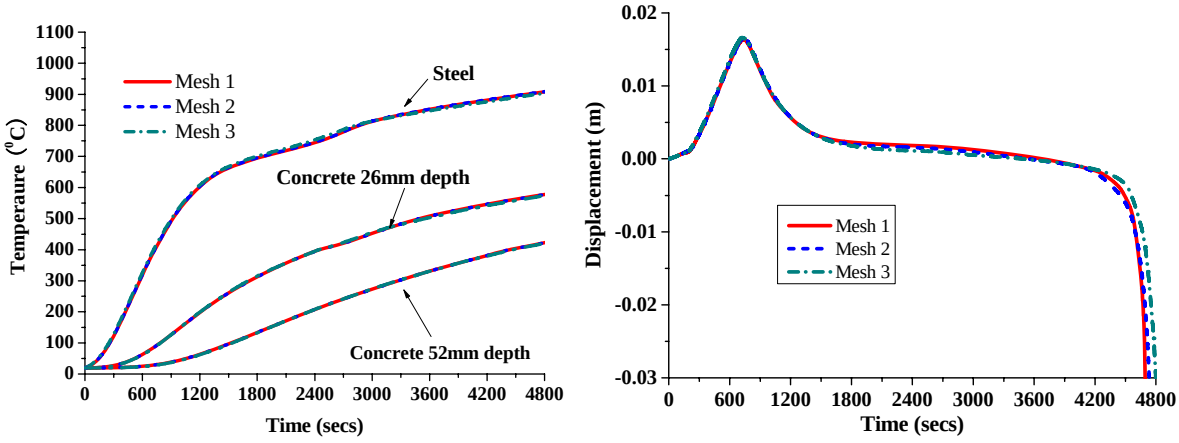

a) Temperature field b) Vertical head displacement

Figure 4: Temperature field and Vertical head displacement using different meshes

2.4 Comparisons with the experimental results

Figures 5-a and 5-b show, respectively, the calculated temperature field and the vertical head displacement of the two columns, where both the time-dependent temperature and the displacements are compared with the test results from Lie and Stringer[7] .

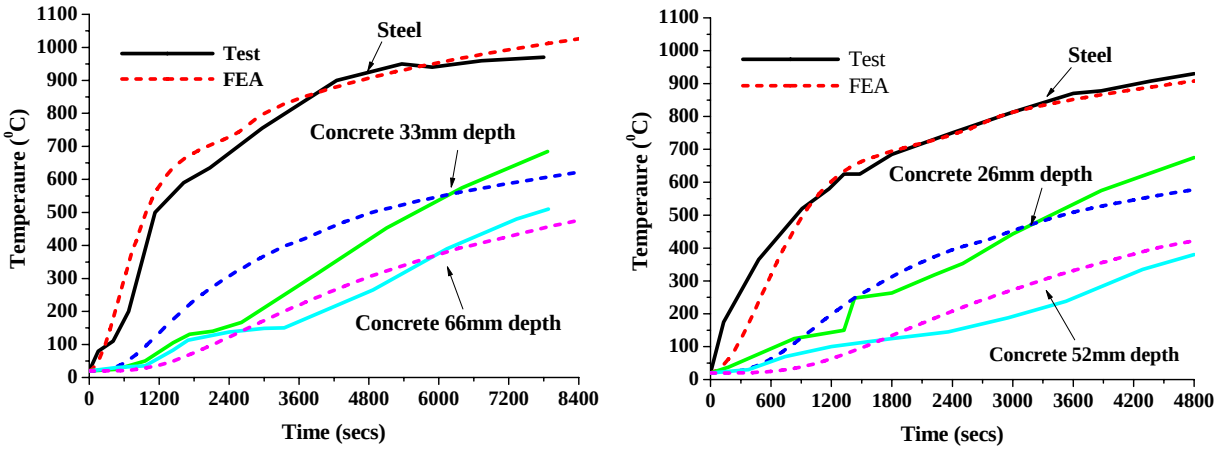

1) Column (a) 273.1mm x 5.56mm 2) Column (b) 219.1mm x 4.78mm

a) Temperature field

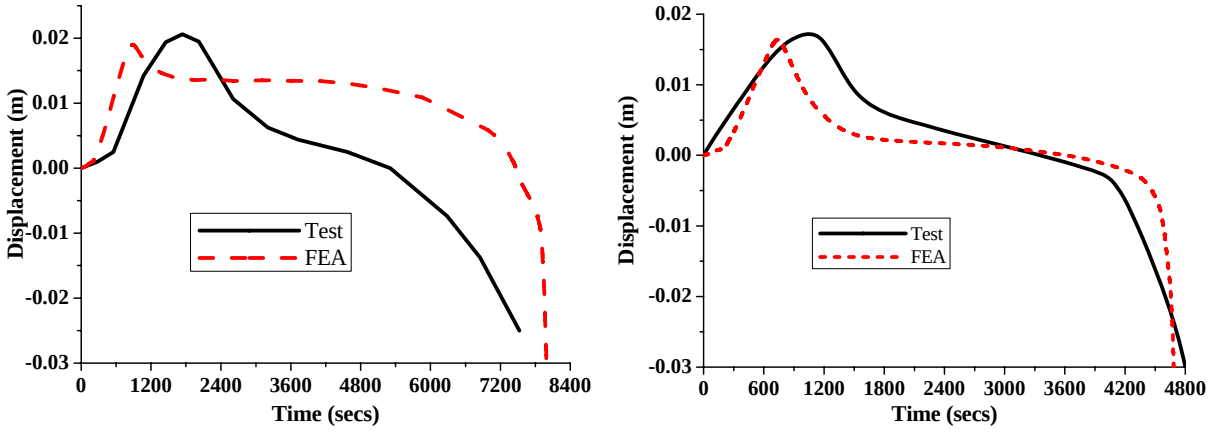

1) Column (a) 273.1mm x 5.56mm 2) Column (b) 219.1mm x 4.78mm

b) Vertical head displacement

Figure 5: Comparison of the temperature field and vertical head displacements

Figure 5-a shows that in general the computed temperature is very close to the test results in the steel, though some notable disagreement occurring in the concrete. Apart from the deviation for using the material properties from various test results, this is also due to the evaporation and flow of water in the concrete that has not been taken into account in the finite element analysis. Although Equation 6 considered the influence of water before and after evaporation, the process of evaporation and its influence on the temperature field are not considered in this finite element analysis. It is observed that the tested temperature curve of concrete is rather flat in the region of 100^{o}C, which is caused by gasification effect of water. Figure 5-b shows the computed fire resistance time and the vertical head displacement of the CFST columns. In general the computed results agree well with those from the test. Though there are discrepancies along the displacement path for many reasons, including those discussed above, the predicted fire resistant time agrees well with the test results. The vertical head displacements of the columns increase to their maximum first, due to the large thermal expansion that overtakes the axial compressive deformation, as the temperature increases, significant reduction of stiffness in both the steel and the concrete results in larger axial compressive deformation that reduces the overall vertical head displacement and leads to the smooth descending displacement path. When the column starts losing its load bearing capacity, a sudden drop of the vertical head displacement occurs. Overall, the predicted displacement path of column (b) agrees better with the test results (Figure 5-b 2), because the computed temperature field of the column is closer to the test temperature.

Additionally, column (b) has a smaller concrete cross section, which may also contribute to the accuracy of the predictions.

After the successful validation, the finite element model is used to carry out a parametric study on the fire resistance of CFST columns as integrated members of a frame. The obtained results and a discussion of them are presented in the following sections.

3 Simulation of frames in fire conditions

In the following simulation of frames in fire, ISO-834 standard temperature-time curve which is similar to the ASTM-E119 standard temperature-time curve is used, since it is the most commonly used fire specification. Further details about these temperature curves can be found in Buchanan[24], (2001). The ISO-834 standard temperature-time curve can be written in the form:

$$T = T_0 + 345\log_{10}(8t + 1) \tag{13}$$

where t is the time in fire; T and T_0, denote, respectively, current and initial temperature of the frames. Again the initial temperature is set to 20^{o}C.

3.1 Simulation model

In order to analyse fire resistance of CFST columns in different frames and at different locations of a frame, the finite element model introduced in Section 2.3.5 is used to study the columns shown in Figure 6, where they act as either integrated members of a frame or independent single columns. In both cases, the columns are subjected to the same fire and mechanical load conditions. The geometric dimension of the frames and the single columns, the applied mechanical loads and the location of fire are also shown in Figure 6.

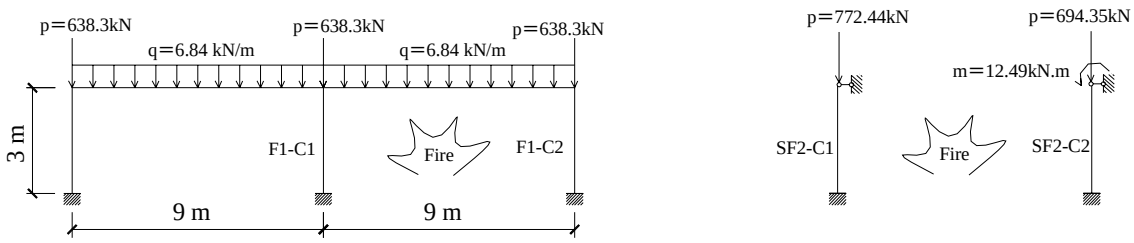

a) Frame-1 b) Single column in Frame-2

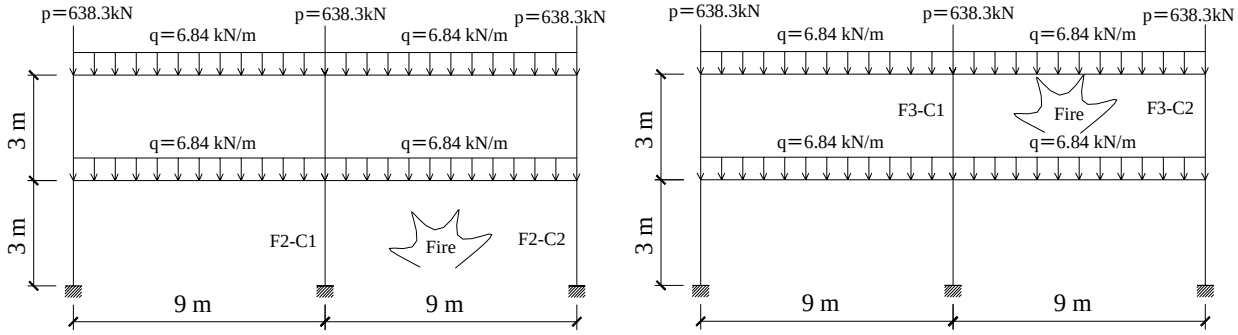

c) Frame-2 d) Frame-3

Figure 6: Computing model of frames in fire

The three frames shown in Figure 6 are all constructed with circular CFST columns and steel beams of I-sections. All the CFST columns have the same section properties, length and are made of the same materials. The height of the column is 3m and the cross-section size is CHS 273×6.3. The I-section steel beam is 356×171×67UB, with a length of 9m. The applied load on the beam is 6.84 kN/m and the axial load on the column is 638.3 kN that is 25% of the maximum bearing capacity of the column at normal temperature (20^{o}C). The single columns, SF2-C1 and SF2-C2 in Figure 6-b, are subjected, respectively, to the same mechanical loads as the two columns, F2-C1 and F2-C2 of Frame-2 shown in Figure 6-c.

In the finite element analysis the failure time and lateral displacement curve of the CFST columns are calculated to evaluate their fire resistance. Since we consider the fire resistance of columns only, it has been assumed that the steel beams have sufficient fire protection and any thermal deformation is negligible in comparison with mechanical one.

3.2 Finite element model of frames

In order to reduce the computer time, solid elements are used only for the columns in fire, while beam elements are used for all beams and columns that are not in fire. To ensure that the columns are rigidly connected to the floor beams, it is assumed that each end of the composite columns is attached to an imaginary rigid plate before it is connected to a beam. Figure 7 is the finite element model of Frame-3. The model of other frames can be built in a similar manner.

The process of simulating the frames in fire is the same as the process described in Section 2.3 for the two test columns.

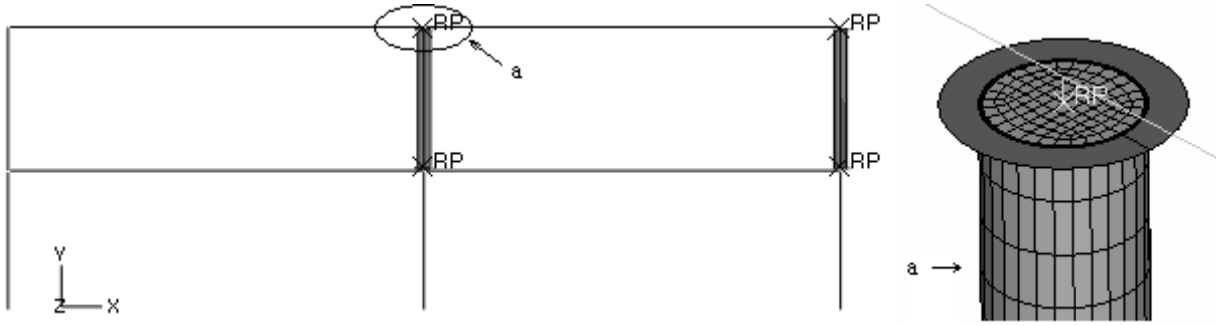

Figure 7: Finite element of Frame-3

For comparisons, two types of fire, i.e. all-round fire and one sided fire are considered in the numerical simulation. For the sake of convenience, the all-around fire and the one-sided fire are named, respectively, as Fire-1 and Fire-2. In Figure 6, only fire on one side of a column is shown. In the following calculations, when referring to all-round fire, it is assumed that a column is attacked by identical fire sources from around the column.

3.3 Collapse analysis of the CFST columns due to buckling

When a column is weakened by fire, which results in redistribution of loads and reduction of material strength and moduli, buckling instability may occur. In this study, the buckling criterions are based on the ISO-834(1989) standard. Buckling occurs when at least one of the following critical stages is reached:

1. The axial decrement of the column reaches to 10H mm.
2. The compressing rate surpasses 3H mm/min.
3. The column can not carry load.

where H is the height of the column in meters.

4 Results and discussions

4.1 The effect of fire types on fire resistance and deformation of CFST columns

Figures 8a and 8b present the temperature distributions along the diameter of the CFST columns

subject to Fire-1 and Fire-2, respectively. The distributions will be used subsequently in the fire resistance studies of the frame columns. It can be seen from the figures that the temperature in the concrete is much lower than in the steel under Fire-1. Under Fire-2 the steel that does not face the fire remains at a relatively low temperature. It can be concluded that the fire resistance of the CFST column in Fire-2 will be higher than that in Fire-1.

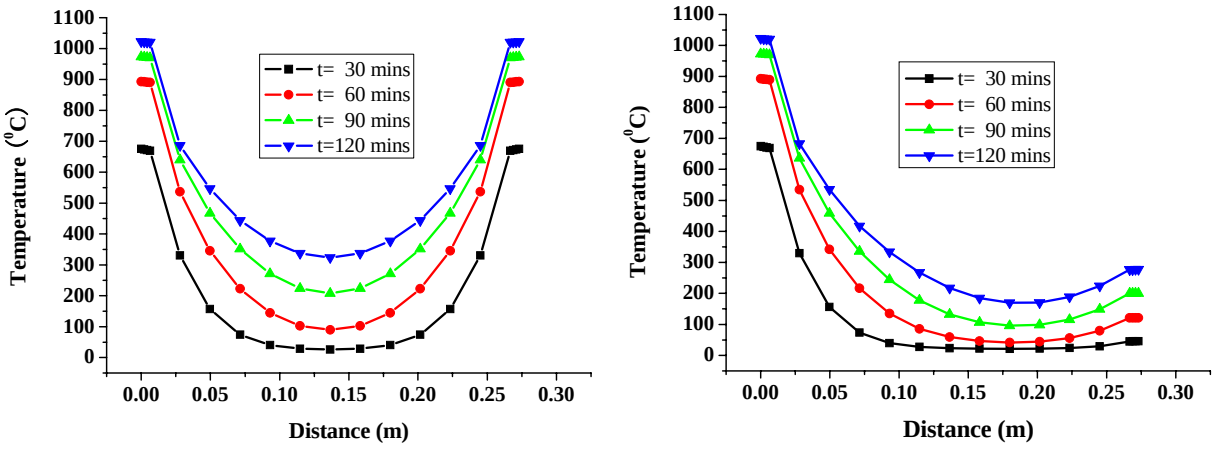

a) Fire-1 b) Fire-2

Figure 8: Temperature along the diameter

Figure 9 shows the vertical head displacement of the columns subject to both types of fire. From this figure it can be found that the fire resistance time of the frame columns under Fire-2 is longer than that under Fire-1, due to the fact that the temperature in the concrete under Fire-2 is much lower than that under Fire-1. The lower temperature in the materials prevents further degradation of stiffness and strength of the column, which exhibits a rather stabilized displacement path for the fire-2 condition. As shown in Figure 10a, where the displacements are taken at 71 minutes for Frame-2 and 76 minutes for Frame-1 and Frame-3, for all round fire, and Figure 10b, where the displacement are taken at 105 minutes for one sided fire, the deformation of the frame columns is also different for the same reasons as argued above.

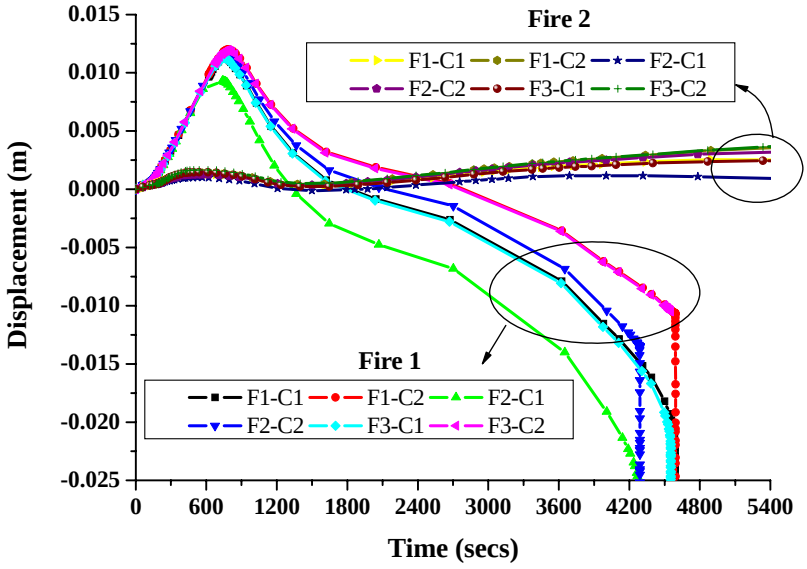

Figure 9: The vertical head displacement of columns in the frames

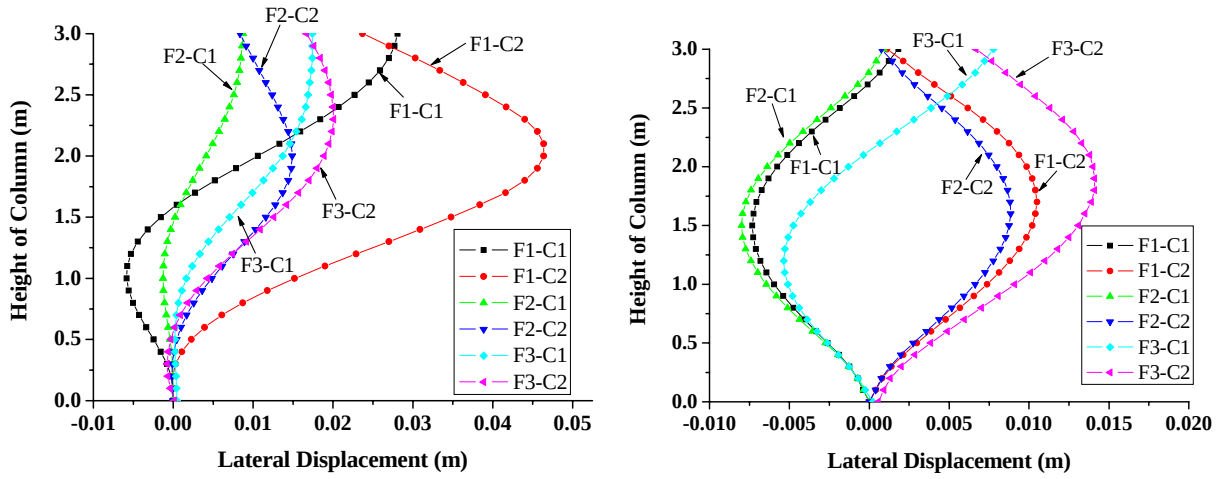

a) Fire-1 b) Fire-2

Figure 10: Lateral displacement of the columns

4.2 The effect of location on the fire resistance and deformation of CFST columns

Two typical column locations, i.e. middle column (F1-C1, F2-C1, and F3-C1) and side column (F1-C2, F2-C2, and F3-C2), are considered for each frame. Within a frame, the columns at the two locations are subjected to different boundary conditions and loads. For example, the axial forces and bending moments acting on the top ends of columns F2-C1 and F2-C2 are, respectively, 772.44kN, 0kN.m and 694.35kN, 12.49kN.m. However, it can be seen from Figure 9 that the two columns have almost identical fire resistance time under Fire-1. Apart from an

almost equal horizontal sway at the top of the two columns, the side columns (F1-C2, F2-C2 and F3-C2) have much big lateral deformation (Figure 10). The CFST columns in the Frame-1 and Frame-3 have the same resistance time (76mins), and both are longer than that of Frame-2 (71mins). This is because the columns of Frame-2 are subjected to greater axial forces.

4.3 The effect of member interaction on the fire resistance and deformation of the CFST columns

In order to evaluation the effect of frame interaction on the fire resistance of the CFST columns, the two columns, F2-C1 and F2-C2, of Frame-2 are studied by considering them first as integrated members of Frame-2. The columns are studied then as isolated columns carrying the same axial forces and moments as they do in Frame-2 (see Figure 6b and 6c). Both types of fire are considered and the vertical head displacements and the lateral displacements of the columns are presented in Figures 11 and 12, respectively.

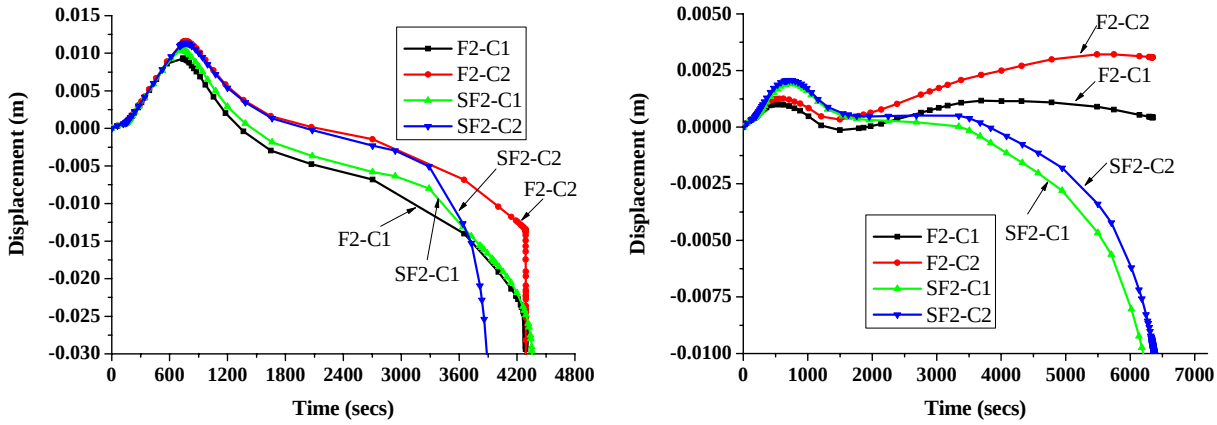

a) Fire-1 b) Fire-2

Figure 11: Vertical head displacement of the single and frame columns

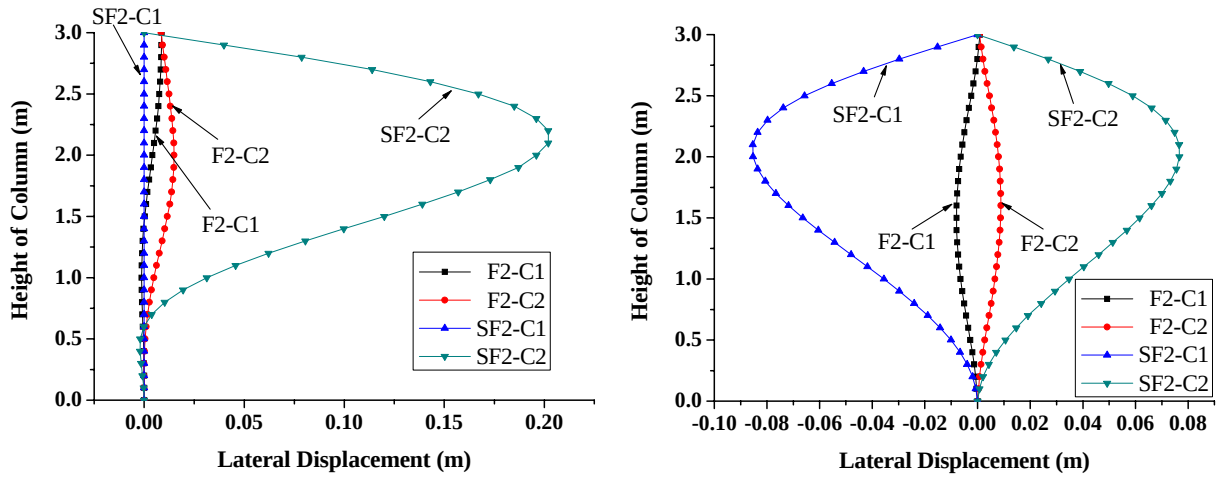

a) Fire-1 b) Fire-2

Figure 12: Lateral displacement of the columns

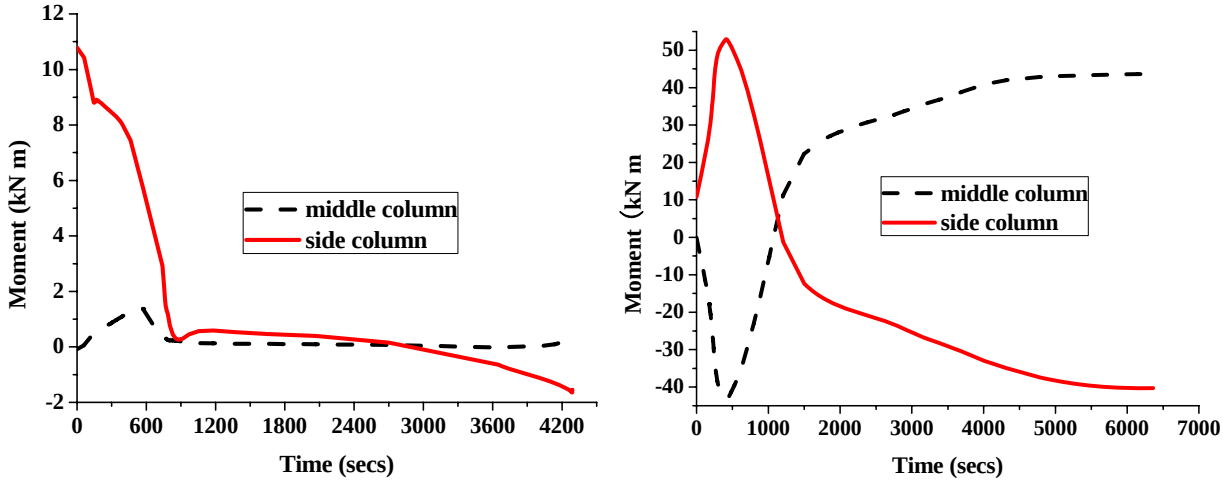

a) Fire-1 b) Fire-2

Figure 13: The culmination moment of the columns in Frame-2

Under Fire-1, the vertical head displacement of the middle column, F2-C1, is very close to that of the single column, SF2-C1, with an almost identical fire resistance time. These are mainly because under the all-around fire the bending moment of the middle column in Frame-2 is negligible. This can be observed from Figure 13a. Thus, the load condition is the same as that of the single column SF2-C1. For the side column of the frame, F2-C2, significant differences in both axial and lateral displacements are observed in comparison with those of the single column, SF2-C2. The frame column F2-C2 has longer fire resistance time. The major reason for this is that as the stiffness of F2-C2 is reduced by the fire, stress redistribution occurs through the

interaction with other members of the frame. Consequently, the bending moment in the side frame column, F2-C2, is significantly decreased, as shown in Figure 13a, and so the axial and lateral displacements are. Because of the reduction in bending moment due to the stress redistribution, the fire resistance of the side column becomes almost identical to that of the middle one. This cannot be observed from the single column analysis, where there is no stress redistribution and the bending moment in SF2-C2 remains unchanged. This results in an overestimated lateral displacement, hence, a shorter fire resistance time.

For the two single columns under Fire-2, the deformations are larger, while the fire resistance times are shorter, than those of their respective frame columns. For the middle columns F2-C1 and SF2-C1, due to the asymmetric distribution of temperature, the stiffness of the column materials close to the fire is reduced and bending of the columns occurs under the action of the axial pressure. It is observed from Figure 13b that after changing the direction of the bending moment, the frame will eventually provide a moment that is opposite to the bending direction of the column and reduced the later displacement. Thus, the single-column model, SF2-C1, overestimates the bending and the lateral deformation since the restrains provided by the floor beams are not presented in the calculation. Consequently, the fire resistance time of the columns are significantly underestimated.

5 Conclusions

The behaviour of CFST frame structures in fire has been investigated by a nonlinear finite element analysis in this paper. The aim of this investigation was to establish a FE model for fire resistance analysis of CFST columns by considering their interactions with floor beams, and to identify conservatism inherited from the traditional design methodologies. The work is important and urgently needed for further development of the performance based fire design method. The main conclusions of this paper are drawn as follows:

1. The manner of a CFST column exposing to a fire, including intensity and direction of a fire, is an important factor in the analysis of its fire resistance because it may lead to additional bending and also a change of bending direction.

2. In a frame system, although middle and side columns may have different end and load conditions, they have almost the same fire resistant time due to stress redistribution.

3. Comparing with single CFST columns subjected to one side fire, the fire resistance of a column member in a frame can be significantly increased because of the redistribution of internal forces in the frame and the restrains from other members. This can be taken into account in a practical design to reduce fire protection costs of columns subject to one side fire.

4. Because of the redistribution of internal forces, the bending moment is significantly reduced in columns subject to Fire-1. In a practical fire safety design, this can also been taken into account to reduce the costs..

5. It is inaccurate to evaluate the fire resistance of an element with fixed design loads, especially fixed bending moment. Accurate simulation of fire test should consider the redistribution of the internal forces and the interaction of the whole structural system. Using the fixed design loads to obtain the fire resistance of an element, e.g., a frame column, will inevitable lead to a conservative design.

6. For a frame, the collapse of a single column does not necessarily represent the collapse of the entire structure. In this paper, however, only 2-span of 2-stored frames are studied, for which collapse of one column is likely to causing collapse of the entire structure. Indeed, further investigation on progressive collapse of multi-stored frame is needed.

Acknowledgement: The second and third authors are grateful to the Royal Society for the financial support (2007/R1-IJP). The authors are also grateful to the reviewers for their constructive comments.

References

1. J. Ding and Y. C. Wang, Finite element analysis of concrete filled steel columns in fire, *Adv. Steel. Struct*. **2** (2005) 1053-1058.
2. D.K. Kim, S.M. Choi and K.S. Chung, Structural characteristics of CFT columns subjected fire loading and axial force. In: *Proceedings of the Sixth ASCCS Conference, Los Angeles, USA* (2000), pp. 271-278.
3. A. K. Kvedaras and A. Sapalas, Research and practice of concrete-filled steel tubes in Lithuania, *J. Constr. Steel. Res*. **49** (1999) 197-212.
4. A. J. O'Meagher, I. D. Bennetts, G. L. Hutchinson and L. K. Stevens, Modelling of HSS columns filled with concrete in fire, BHPR/ENG/R/91 /031/ PS69, Melbourne, Australia (1991).
5. T. Okada, T. Yamaguchi, Y. Sakumoto and K. Keira, Load heat tests of full-scale columns of concrete-filled tubular steel structure using fire-resistant steel for buildings. In: *Proceedings of the Third International Conference on Steel–Concrete Composite Structures (I)*, ASCCS, Fukuoka (1991), pp. 101–106.
6. T. T. Lie, Fire resistance of circular steel columns filled with bar-reinforced concrete, *J. Struct. Eng.-ASCE.* **120**(5) (1994) 1489-1509.
7. T. T. Lie and D. C. Stringer, Calculation of the fire resistance of steel hollow structure section columns filled with plain concrete, *Can. J. Civil. Eng*. **21**(3) (1994) 382-385.
8. V. K. R. Kodur, Performance-based fire resistance design of concrete-filled steel columns, *J. Constr. Steel. Res*. **51**(1) (1999) 21-26.
9. V. K. R. Kodur and M. A. Sultan, Enhancing the fire resistance of steel columns through composite construction, In: *Proceedings of the Sixth ASCCS Conference, Los Angeles, USA* (2000), pp. 279-286.
10. Y. C. Wang, Some considerations in the design of unprotected concrete-filled steel tubular columns under fire conditions, *J. Constr. Steel. Res*. **44**(3) (1997) 203-223.
11. Y. C. Wang, A simple method for calculating the fire resistance of concrete-filled CHS columns, *J. Constr. Steel. Res*. **54** (2000) 365-386.

12. X. X. Zha, FE analysis of fire resistance of concrete filled CHS columns, *J. Constr. Steel. Res*. **59** (2003) 69–779.
13. S. Liu, Y. Li, X. X. Zha and J. Q. Ye, The Non-linear Simulation of the Behaviour of Integral Concrete-Filled Steel Tubular Framed Structures in Fire Conditions, In: *Proceedings of the Tenth International Conference on Civil, Structural and Environmental Engineering Computing*. (Civil-Comp Press, Rome, Italy, 2005).
14. J. Yin, X. X. Zha and L. Y. Li, Fire resistance of axially loaded concrete filled steel tube columns, *J. Constr. Steel. Res*. **62** (2006) 723-729.
15. L. H. Han, Fire performance of concrete filled steel tubular beam-columns, *J. Constr. Steel. Res*. **57**(6) (2001) 695-709.
16. L. H. Han, L. Xu and X. L. Zhao, Tests and analysis on the temperature field within concrete filled steel tubes with or without protection subjected to a standard fire, *Adv. Struct. Eng*. **6**(2) (2003a) 121-133.
17. L. H. Han, Y. F. Yang and L. Xu, An experimental study and calculation on the fire resistance of concrete-filled SHS and RHS columns, *J. Constr. Steel. Res*. **59**(4) (2003b) 427-452.
18. L. H. Han, X. L. Zhao and Y. F. Feng, Experimental study and calculation of fire resistance of concrete-filled hollow steel columns, *J. Struct. Eng.-ASCE*. **129**(3) (2003c) 346-356.
19. The University of Edinburgh. Final report of the DETR-PIT project: Behaviour of steel framed structures under fire conditions. *Technical report, The University of Edinburgh*, 2000.
20. Y. C. Wang, The effects of structural continuity on the fire resistance of concrete filled columns in non-sway frames. *J. Constr. Steel. Res*, **54**(2) (1999) 177-197.
21. Y. Li, Study on fire resistance of concrete-filled steel tubular columns in frame, MSc thesis, *Huazhong University of Science and Technology*, Wuhan, China (2006). (In Chinese)
22. European Committee for Standardization, EN 1994-1-2:2005, Design of composite steel and concrete structures Part 1.2: general rules, structural fire design. (Brussels, 2005).
23. J. Duan, Z. H. Xiang and M. D. Xue, Thermal-dynamic coupling analysis of large space structures considering geometric nonlinearity, *Int. J. Struct. Stab. Dy*. **8**(4) (2008) 569-596.

24. A. H. Buchanan, Structural design for fire safety. (John Wiley & Sons, New York, 2001).